Review

Recent developments in the chemistry of stable silylenes

Nicholas J. Hill, Robert West *

Department of Chemistry, Organosilicon Research Center, 1101 University Avenue, University of Wisconsin-Madison, Madison, WI 53706, USA

Abstract

This paper reviews progress in the field of thermally stable silylenes since 2000. Developments in the synthesis and characterization of new stable silylenes are discussed, followed by a summary of recent theoretical calculations upon model silylenes. The main part of the article concerns the reactivity patterns displayed by silylenes **1–4**, which are discussed in terms of their behavior toward radical, organic, inorganic, and organometallic species.
© 2004 Elsevier B.V. All rights reserved.

1. Introduction

Silylenes are divalent, dicoordinate silicon species which, until recently, were only observable at low temperatures [1]. The *N*-heterocyclic silylenes **1–3**, silicon analogues of the Arduengo *N*-heterocyclic carbenes [2], were first reported during the mid-1990s (Scheme 1) [3]. These molecules are stable at room temperature under anaerobic conditions (**2** exists as a *Z*-diaminodisilyldisilene in the solid state) [4] and benefit both from electronic stabilization by the amino groups and steric protection by the bulky alkyl groups. For **1** and **3**, additional stabilization is provided by aromatic π-electron delocalization over the silicon-containing ring. Since their isolation several theoretical studies have examined aspects of structure and bonding in **1–3**, and their reactivity toward a range of organic, inorganic and organometallic substrates continues to be explored. The current article aims to summarize developments in stable silylene chemistry since the area was initially reviewed in 2000 [5,6].

2. Synthesis and structure

In 1999, Kira et al. [7,8] reported the synthesis of the first isolable dialkylsilylene **4**. Prepared by reductive debromination of the precursor dibromosilane, this species is distinct from **1–3** in that its stability is derived entirely from steric protection of the divalent silicon atom by two SiMe$_3$ groups attached to the α-carbons. **4** is monomeric in the solid state and stable at 0 °C but slowly converts to the silacyclopentene **4a** in solution at room temperature via an intramolecular 1,2-migration of a SiMe$_3$ group to the silicon atom. **4a** is the first example of a cyclic silene (see Scheme 2).

Of note is the very low-field ^{29}Si NMR signal of 567 ppm for **4**, compared to the calculated values of 771.8 ppm for H$_2$Si: and 739.6 ppm Me$_2$Si:, and the experimental values of 78.3, 118.3, and 96.9 ppm for **1**, **2**, and **3**, respectively. The UV–Vis band maximum due to the n(Si) → 3pπ(Si) transition in **4** was observed at 440 nm ($\varepsilon = 500$), close to that for dimethylsilylene (450 nm). In comparison, the equivalent transition for **3** is observed at 344 and 302 nm for **3a**. Taken with the ^{29}Si NMR data, this indicates that the electronic environment of the silicon atom in **4** is more akin to the dicoordinate, divalent silicon in transient silylenes than that of the *N*-stabilized silicon atom in **1–3**.

* Corresponding author. Tel.: +1 608 262 1873; fax: +1 608 262 6143.
E-mail address: west@chem.wisc.edu (R. West).
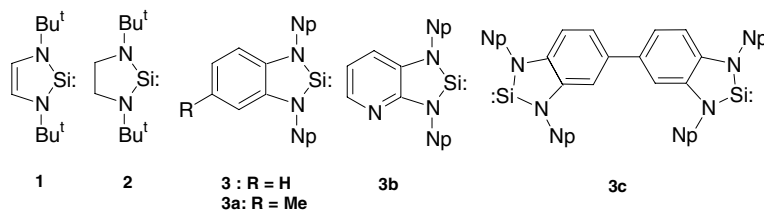
Scheme 1.
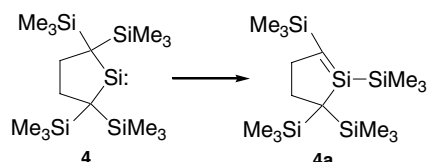
Scheme 2.

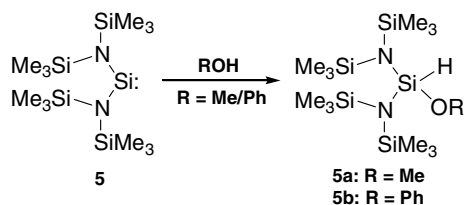The synthesis of the acyclic bis(amino)silylene [(Me₃Si)₂N]₂Si: (**5**), the silicon analogue of the familiar germanium and tin compounds first described in the mid-1970s [9], was recently reported [10]. **5** is an orange-red substance which persists in solution at −20 °C but decomposes to uncharacterized products near room temperature, and displays a ^{29}Si NMR signal of 224 ppm (at −20 °C), a value which lies between those obtained for **1–3** and **4**. Reaction of **5** with MeOH and PhOH gave the trapping products **5a** and **5b**, respectively (see Scheme 3).

Density functional theory (DFT) calculations indicate that **5** is less stable than [(Me₃Si)₂N]₂Ge: and [(Me₃Si)₂N]₂Sn: by ca. 73 and 130 kJ mol^{-1}, respectively. These calculations also predict **5** to be monomeric in solution, with the bulky SiMe₃ groups preventing dimerization [10].

Gehrhus has further demonstrated the importance of large, sterically demanding N-substituents for the stability of silylenes [11]. The potassium reduction of **3d**, an analogue of **3** where the *neo*-pentyl groups are replaced by ethyl groups, resulted not in the isolation of a stable *N*-heterocyclic silylene but of the thermally stable cyclotetrasilane radical anion **6**$^{-\cdot}$ and a similar dianion **7**$^{2-}$ (Scheme 4).

The Si–Si bond distance in **6**$^{-\cdot}$ (2.347(2) Å) is slightly shorter than that typically found in cyclopolysilanes, while the equivalent distance in **7**$^{2-}$ is 2.284(2) Å. The latter value is comparable to the Si=Si bond length of 2.289(2) Å in the *Z*-diaminodisilyldisilene [4] (the solid-state form of **2**) and is only slightly longer than the upper bound for typical Si=Si bonds (ca. 2.14–2.26 Å). The short bond lengths are rationalized in terms of delocalization of one (for **6**$^{-\cdot}$) or two (for **7**$^{2-}$) electrons around the planar Si₄ ring, in agreement with both simulated and observed EPR spectra of the radical anion ($g = 2.0025$, $a(^{29}\text{Si}) = 3.5$ G). **6**$^{-\cdot}$ exists as a solvent separated ion pair, while the solvated potassium cation in **7**$^{2-}$ is weakly η²-bound to the phenyl ring. Similar results were obtained with the *iso*-butyl substituted species [11].
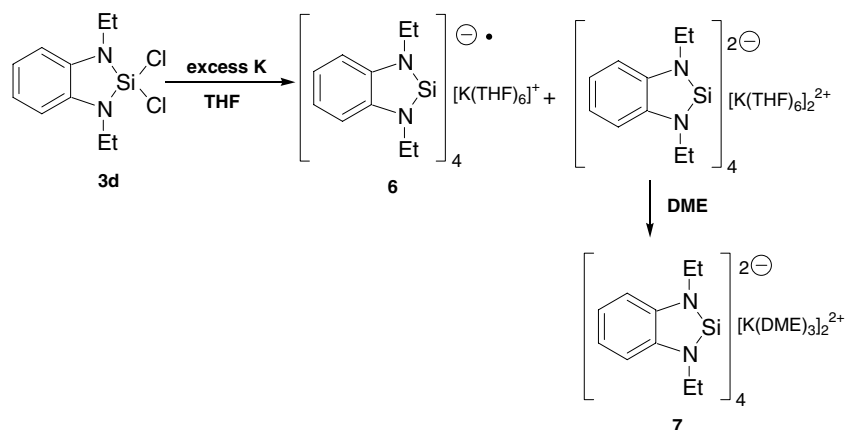
Scheme 3.

Scheme 4.

Attempts to isolate modified versions of **1** bearing phenyl, *p*-tolyl, mesityl, or adamantyl substituents in place of *tert*-butyl have so far been unsuccessful, generating a complex mixture of inseparable products [12]. Heinicke et al. [15a] isolated the pyrido-fused silylene **3b** (^{29}Si NMR = 95.1 ppm) and synthetic, spectroscopic, and X-ray structural details have been outlined for **3c** [5a], which represents the first example of a thermally stable bis-silylene (^{29}Si NMR = 96.6 ppm). Theoretical and chemical reactivity studies have yet to be described for either of these compounds. A similar situation exists for the 2,6-(di-isopropyl)phenyl-substituted analogue of **1**, which was reported in 1998 (^{29}Si NMR = 76.8 ppm) [14]. In related work the cyclic silylene **8**, a silaazaanthracene derivative, was generated by lithium naphthelenide reduction of the precursor dichloride at −78 °C in the presence of excess isoprene or 2,3-dimethylbuta-1,3-diene [15]. The expected trapping products **8a** and **8b** were obtained, although no silylene was isolated following similar reduction in the absence of a trapping agent (Scheme 5). Furthermore, UV–Vis bands due to **8** were not observed at −78 °C, indicating that the silylene is not stable even at low temperature. Hence, the steric protection provided by the *tert*-butyl (for **1** and **2**), *neo*-pentyl (for **3a**–**c**), or trimethylsilyl (for **4**) substituents appears to be the minimum required for isolation of a thermally stable silylene.

The low-temperature X-ray crystal structure of **1** reveals the molecule to exist in the orthorhombic space group *Pmmn* [16,17]. **1** is planar and isostructural with the analogous *N*-heterocyclic germylene [18] and displays no intermolecular interactions. The packing diagram is shown in Fig. 1. The structure of **1** was initially established by gas-phase electron diffraction data [3a].

3. Theory

The unsaturated silylenes **1** and **3** contain five-membered rings with six π electrons, and so may be considered as aromatic species. Aromatic stabilization in **1** was originally controversial [19], but by 2000 was relatively well established by several experimental and theoretical studies. Among these were isodesmic calculations [20] and nucleus-independent chemical shift calculations [21] both indicating the aromatic res-
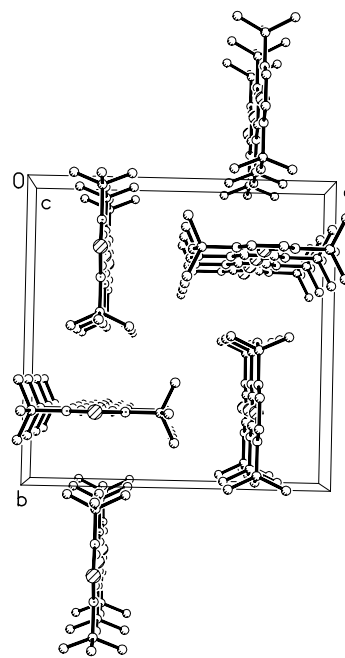

Fig. 1. Packing diagram for **1**. Reprinted from [16]. Copyright Freund Publishing.

onance energy in **1** to be about 50–60% of that in benzene.

Recent experiments and theoretical computations confirm this view. The Raman spectrum of **1** has been studied and compared with that for analogous compounds with tetrahedral silicon atoms such as **1-Cl$_2$**, where no cyclic delocalization is possible. The C=C stretching mode in **1** is enhanced many hundredfold over that for the non-aromatic reference compounds [22], a strong indication of extensive conjugation in **1** [23]. Similar studies suggest that π-delocalization is even greater in the germanium analog of **1** [24].
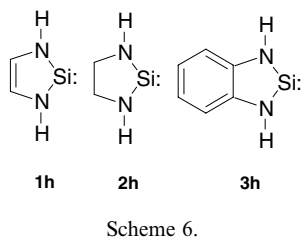
New calculations of the enthalpy of isodesmic reactions

$$LSi: + SiH_4 = LSiH_2 + H_2Si:$$
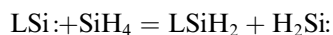
have been carried out by Oláh and Veszprémi [25]. The ΔE values are calculated to be 51.5 and 38.9 kcal mol^{-1} for **1** and **2**, respectively. The difference of 12.6 kcal mol^{-1} can be ascribed to the aromatic stabilization energy of **1**.

Scheme 5.

Scheme 6.

Fig. 2. Shielding tensor components for R_2Si:.
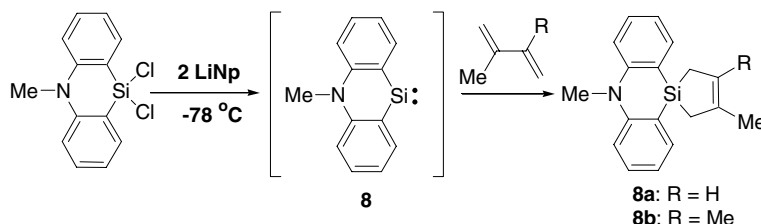
The stability of silylenes is related to the singlet–triplet splitting energy, ΔE_{S-T}. For the model molecule **1h** (Scheme 6), three values for ΔE_{S-T} have been reported, 65.3, 59.7 [26] and 59.3 kcal mol^{-1} [25], depending on the level of theory employed.

An interesting result is that ΔE_{S-T} is predicted to be greater for the non-conjugated **2h** (75.5 kcal mol^{-1}) than for **1h** (59.3 kcal mol^{-1}). For both **1h** and **2h** the ΔE_{S-T} values are much higher than for unstabilized silylenes such as SiH_2 (20.1), $HSiCH_3$ (22.3) and **4** (32.4). The singlet–triplet splittings are related to the energy of dimerization to a $Si{=}Si$ compound (a disilene), which is strongly exothermic for simple silylenes but endothermic for **1h** and **2h** [23]. The same group has reported elaborate calculations of spin-philicity and spin-donicity for stable silylenes, carbenes and germylenes [27]. The sum of the spin potentials correlates well with the vertical ΔE_{S-T} values. In another study, the relative stability of **1h** and the 14 other five-membered ring isomers of this molecule have been investigated theoretically; **1h** was found to be the most stable of all, even though some other isomers showed greater aromaticity according to isodesmic reactions [28].

A detailed theoretical study of the chemical shift tensors of silylenes has been reported by Müller [29]. For all silylenes the shielding tensor is highly anisotropic, with a large paramagnetic eigenvalue δ_{11} in the plane of the central R–Si–R unit and perpendicular to its C_2 axis (Fig. 2).

The calculations indicate that a paramagnetic contribution from the lone pair on silicon dominates the tensor, leading to very large deshielding. For example, the tensor components for H_2Si: are 2095, 417, and -196 ppm (δ values) giving a predicted isotropic chemical shift of 771.8 ppm. However, the shielding tensor is greatly influenced by substituent and steric effects. π-donor substituents like nitrogen release charge into the silicon p-orbital, destabilizing it and greatly reducing $\delta_{11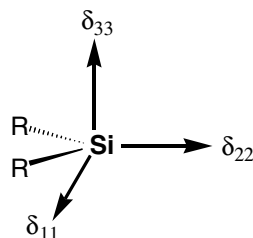}$. In **1**, for example, the tensor components measured by solid state NMR spectroscopy are 284.9, -16.1, and -43.3 ppm, giving an isotropic chemical shift of 75.2 ppm. These results explain why the isotropic chemical shifts for **1–3** are relatively small, while that for **4** is much more deshielded [7]. The crucial δ_{11} term for silylenes is determined by the energy difference between the S_0 ground state and the S_1 excited state. Therefore, a nearly linear relationship is found between the isotropic chemical shifts and the electronic absorption maxima.

A DFT study by Pause et al. [30] reports the geometries of model molecules for stable silylenes, germylenes and carbenes. Using a complex cycle calculation, reduction potentials were estimated to be -2.97 V for **1h** and -2.88 V for **3h**, vs. SCE. Large negative reduction potentials undoubtedly are important in allowing stable silylenes to be synthesized in the presence of very vigorous reductants like potassium metal.

Electron affinities and ionization potentials, as well as geometries, have also been calculated for **1** and **2** by DFT methods [31]. Results are shown in Table 1, together with experimental values of ionization potentials from photoelectron spectroscopic measurements. Agreement between the calculated and measured values is quite good.

The electrochemical properties of **1** and **2** have been studied by cyclic voltammetry [29]. Silylene **1** shows an oxidation wave at 0.67 V (vs. Ag/AgCl) and a reduction at -2.67 V; **2** displays an oxidation wave at 0.95 V and *two* reduction waves at -1.75 and -2.35 V. The latter result is consistent with the finding that **2** (but not **1**) can be chemically reduced to either a silyl or disilanyl dianion [62]. The voltammetric waves are all irreversible, and the oxidation peaks do not correlate with the ionization potentials, probably because of kinetic and surface effects.

Several papers have appeared concerning unknown but possibly stable silylenes. Earlier Veszprémi et al.

Table 1
Calculated electron affinities and ionization potentials for silylenes

Compound	E_A		I_p		Exp. [18,32]
	Vertical	Adiabatic	Vertical	Adiabatic	
1	0.73	0.70	6.98	6.70	6.96, 7.13, 7.23
2	0.64	0.50	7.30	7.10	7.54
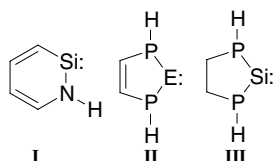
Scheme 7.

[33] calculated the relative stability of six-membered rings containing silicon and nitrogen atoms. Relatively high stability was found for silylene **I** (Scheme 7), for which an aromatic stabilization energy of 14.7 kcal mol^{-1} was calculated from an isodesmic reaction, compared with 28.2 kcal mol^{-1} for benzene in a similar reaction. According to these calculations **I** should have similar stability to **1h**. Molecules based on structures related to **I** were proposed as synthetic targets, but so far none have been reported. Veszprémi's [34] ideas on stable silylenes have been augmented in a recent review.
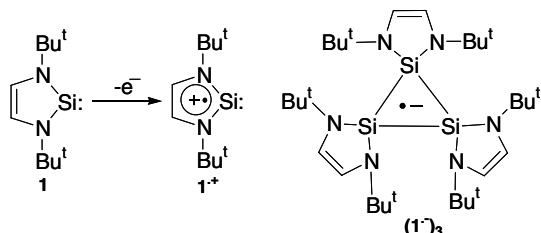
Schoeller and Eisner have carried out calculations on molecules of type **II**, in which phosphorus atoms take the place of the nitrogens in the ring (Scheme 7) [35]. The authors suggest that **III** might be a good candidate for synthesis. However, the stabilization in the phosphorus-containing silylene may be much less than for **1**, since the singlet–triplet separation energy for **III** was calculated to be only 34 kcal mol^{-1}, compared with 53.9–65.3 kcal mol^{-1} for **1**.

4. Chemical reactions

4.1. Reactions involving radical species

Silylenes **1**, **2**, and **4** have displayed some unusual and unexpected radical chemistry. In this section, the reactivity of these species with or as radicals is surveyed. The only example of the radical chemistry of **3** appears to be the previously discussed cyclotetrasilane radical anion **6$^{-\cdot}$** [11].

A combined electrochemical and EPR study of the oxidation of **1** provides direct spectroscopic evidence for the existence in solution of the radical cation **1$^{+\cdot}$** ($t_{1/2} \approx 10$ min at 20 °C, $g = 2.0017$) (Scheme 8) [36]. The EPR spectrum of **1$^{+\cdot}$** shows hyperfine coupling (*hfc*) of the unpaired electron to two equivalent hydro-
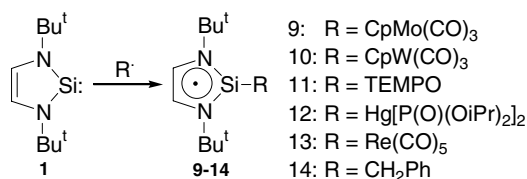
gens and two equivalent nitrogen atoms ($a(^1H) = 8.63$ G, $a(^{14}N) = 2.83$ G) in agreement with the simulated spectrum, suggesting that the radical is delocalized about the C_2N_2Si ring. EPR data obtained following electrochemical reduction of **1** show *hfc* to six nitrogen and three silicon atoms ($g = 2.0035$, $a(^{29}Si) = 25.77$ G, $a(^{14}N) = 1.3$ G) suggesting the existence of a cyclotrisilane anion radical (**1$^{-\cdot}$**)$_3$ ($t_{1/2} \approx 30$ s at 20 °C) rather than the simple radical anion **1$^{-\cdot}$** (Scheme 8). The higher steric demand of the *tert*-butyl group compared to the *neo*-pentyl group may prevent formation of a cyclotetrasilane analogous to **6$^{-\cdot}$** [11].

The reaction of **1** with a range of organometallic and organic radical sources has been studied by EPR spectroscopy [37]. Addition of [CpM(CO)$_3$]$_2$ (M = Mo, W), TEMPO (TEMPO = 2,2,6,6-tetramethylpiperidine *N*-oxide), or Hg[P(O)(OPr-*i*)$_2$]$_2$ to a toluene solution of **1** at 298K, or UV irradiation of a solution of **1** containing Re$_2$(CO)$_{10}$, led to the formation of the mono-radical adducts **9–13** (Scheme 9). These adducts show significant *hfc* with the ^{14}N and ^1H atoms of the silylene ring (for example, **9**: $g = 2.0027$, $a(^1H) = a(^{14}N) = 5.7$ G; **11**: $g = 2.0049$, $a(^1H) = 6.3$ G, $a(^{14}N) = 5.2$ G) indicating that, in each species, the unpaired electron is delocalized over the five-membered ring of the silylene moiety as observed for **1$^{+\cdot}$**. Typical EPR spectra are shown in Fig. 3.

Similar reaction of **2** with [CpW(CO)$_3$]$_2$ gave the [C$_2$N$_2$Si=WCp(CO)$_3$]$^\cdot$ radical but in this case aromatic delocalization cannot occur and the unpaired electron is localized at the tungsten atom, with no ^{14}N or ^1H coupling observed. Although EPR data for **9–13** reveal isotropic hyperfine coupling of the electron with the ^1H-, ^{14}N-, ^{31}P-, and $^{185/187}Re$-nuclei, similar coupling was not observed with the ^{29}Si nucleus in any of the adducts. UV irradiation of a toluene solution of **1** gave rise to **14**, arising from combination of **1** with a benzyl radical formed in situ. EPR data obtained at 298K indicate that the electron is delocalized about the C_2N_2Si ring, as for **9–13**, but at 225K the ^{14}N multiplet broadens and at 195K only a quintet remains. DFT calculations upon **14** and the model radical **14a** (CH$_2$Ph and *tert*-butyl groups replaced by Me) suggest that the rate of conversion between the two conformations of the radical is insufficient to cause an averaging of the *hfc* values for ^{29}Si at room temperature. Hence, the low temperature

Scheme 8.

9: R = CpMo(CO)$_3$
10: R = CpW(CO)$_3$
11: R = TEMPO
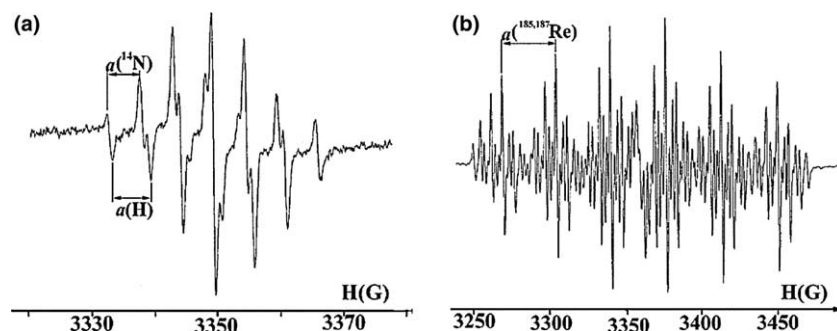12: R = Hg[P(O)(OiPr)$_2$]$_2$
13: R = Re(CO)$_5$
14: R = CH$_2$Ph

Scheme 9.

Fig. 3. Experimental EPR spectra of radical adducts (a) **11** and (b) **13** [37].

broadening and lack of ^{29}Si satellite lines in the EPR spectra of the radical adducts **9**–**14** is probably due to conformational interconversion [37].

Reaction of **1** with TEMPO on a preparative scale yields the trisiloxane **15** as the major product (Scheme 10) [38]. The reaction is thought to proceed via the aminosiloxyl radical **11**. This species may either add another molecule of TEMPO to give the 1:2 adduct **11a**, or undergo O–N bond cleavage to produce the transient silanone **11b**. Combination of **11a** and **11b** gives the observed product **15**.

Treatment of **1** with ^{t}BuO·, formed in situ from thermolysis of ^{t}BuO–OBu^{t}, leads to an approx 85:15 mixture of the 1:2 adduct **17** and the unusual trisilane **19** (Scheme 11) [38]. A likely pathway for these products is shown in Scheme 11. The initial radical adduct **16** may add another ^{t}BuO· radical to form **17**, or may react with **1** to give the intermediate **18**. The latter then reacts with **16** to give the trisilane **19** (Fig. 4).

The reaction of **4** with TEMPO produced the 1,3-disiladioxetane **20** and 2,2,6,6-tetramethylpiperidine, whereas reaction of TEMPO with the germanium and tin analogues of **4** yielded the 1:2 adducts **21** (Scheme 12) [39]. The 1:1 radical adduct **4b** was suggested for all three metalylenes, with O–N bond scission in the silicon radical yielding a transient silanone which dimerizes to give **20**. Cleavage of the O–N bond is evidently too rapid to compete with the addition of a further
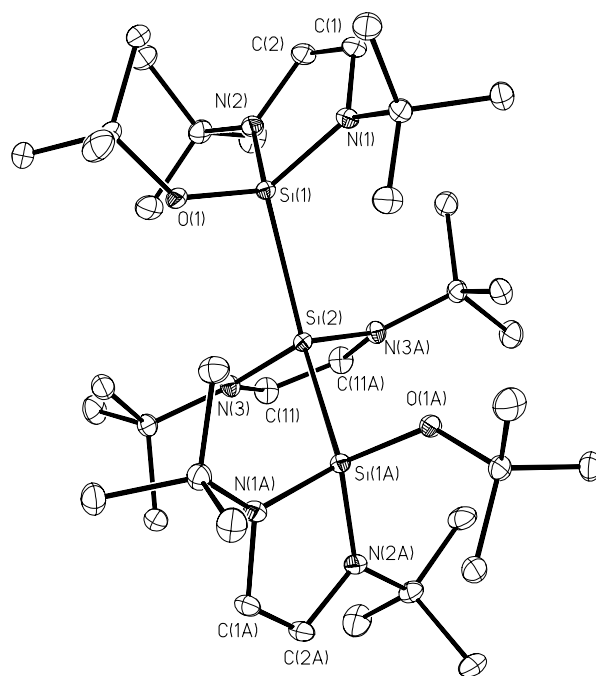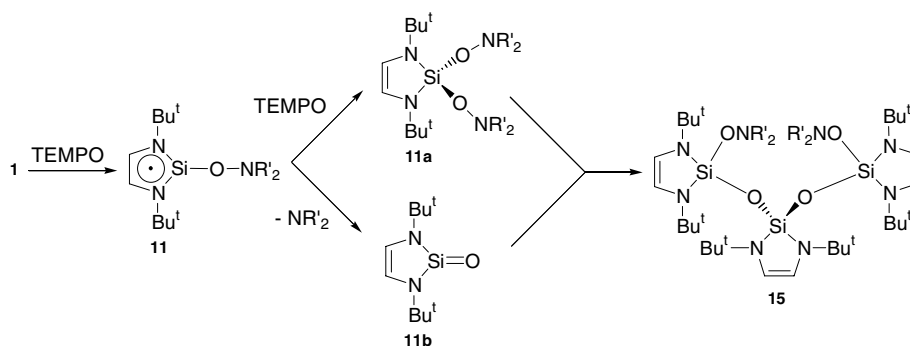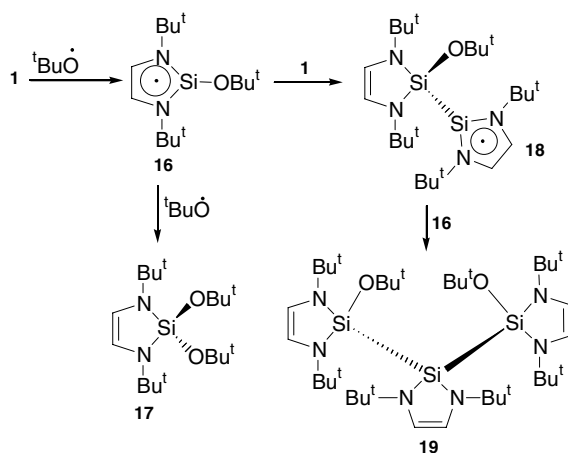

Fig. 4. Crystal structure of **19** [38].

TEMPO radical to give the 1:2 adduct. In contrast, the 1:1 germoxy and stannoxy radical adducts simply couple with a further molecule of TEMPO to give the observed 1:2 adducts **21**. DFT calculations indicate that

Scheme 10.

Scheme 11.

O–N bond cleavage is slightly exothermic in the siloxyl radical but strongly endothermic for the corresponding germanium and tin species [40]. Stable 1:2 adducts were obtained from the reaction of TEMPO with the germanium analogs of **1** and **2** [38].

A series of reactions of **1** with haloalkanes were recently reported in which the products obtained were strongly dependant upon the structure of the alkyl halide substrate [41]. For example, addition of CCl$_4$ to a hexane solution of **1** at room temperature immediately gave the yellow disilane 2:1 adduct **22**, whereas similar treatment of **1** with the bulkier *tert*-butyl chloride led exclusively to the 1:1 adduct **23**, resulting from insertion of **1** into a C–Cl bond (Scheme 13).

These observations were initially rationalized in terms of a halophilic mechanism (a common reaction pathway for phosphanes, which are isolobal with silylenes), where attack of **1** at the halogen atom of the substrate formed a weak 1:1 acid–base complex **1a** (Scheme 14). The steric demand of the halocarbon was assumed to determine the product formed since, with smaller substrates, the electron-deficient silicon atom may accept the lone pair from a second molecule of **1** into its vacant p-orbital (**1b**), followed by a 1,3-shift to form the disilane **22a**. However, with more sterically demanding halocarbons,

1a is too hindered to allow the close approach of a second molecule of **1** and thus a 1,3-shift to give the disilane is not possible. The 1:1 insertion product **23a** might then arise from a 1,2-shift in the intermediate complex, or by single-electron transfer and radical combination. Similar results were obtained from reaction of **2** with a range of haloalkanes.

With bromobenzene, both the 2:1 disilane **22b** and the 1:1 insertion product **23b** are obtained in a slow process (ca. 5 h), the proportion of these products depending on the ratio of the reactants; a fourfold excess of bromobenzene exclusively yields **23b** (Scheme 15). Formation of **22b** was not observed upon treatment of **23b** with excess **1**, even upon heating.

DFT calculations on the reaction of a model cyclic bisaminosilylene with CH$_3$Cl and CHCl$_3$ have questioned the validity of the proposed halophilic mechanism [42,43]. In these studies the putative acid–base complexes analogous to **1b** are either not predicted or found to be thermodynamically insignificant. A three-step mechanism is anticipated instead, where an initial donor–acceptor intermediate **1c** is formed through donation of the halogen lone pair into the vacant p-orbital of the silylene followed by insertion of the silylene into the C–Cl bond via a three-membered transition state to give the 1:1 insertion product **1d**. Insertion of a further silylene molecule, via another cyclic transition state, leads to formation of the disilane **22h** (Scheme 16).
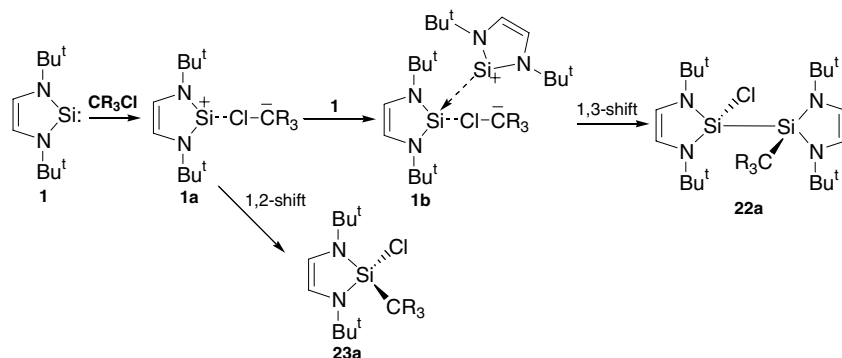
However, this mechanism presents several problems. Chief among these is the high calculated activation energy (≈220 kJ mol^{-1}) for the formation of the initial three-membered transition state leading to **1d**. Such a thermodynamic barrier is inconsistent with the experimental
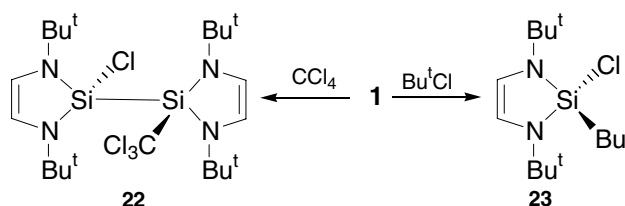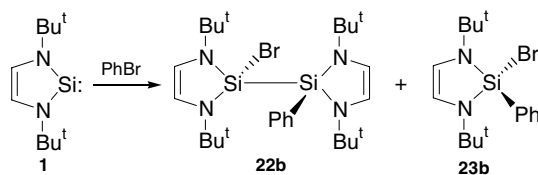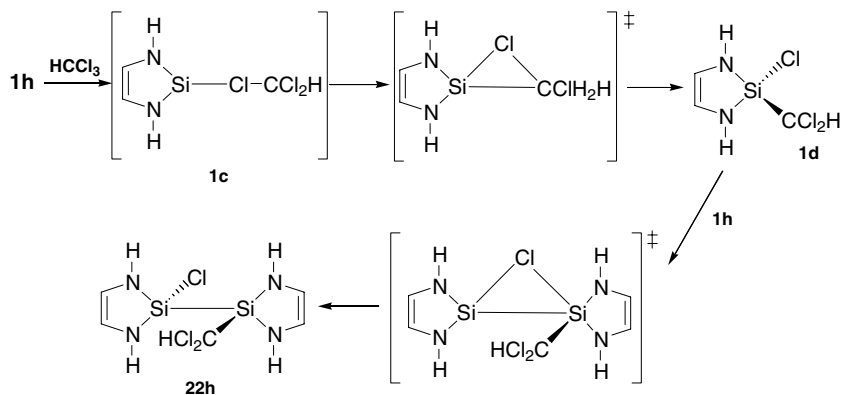

Scheme 13.
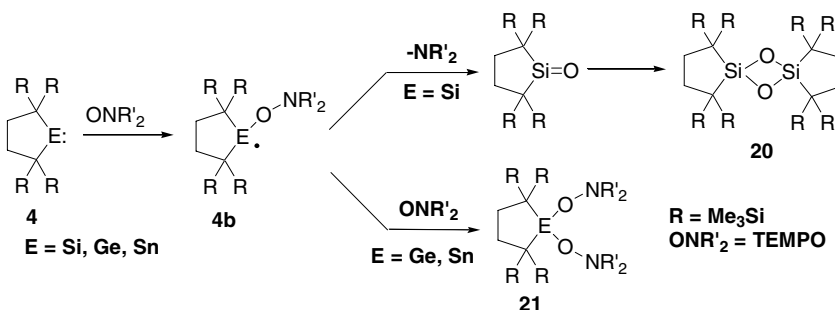
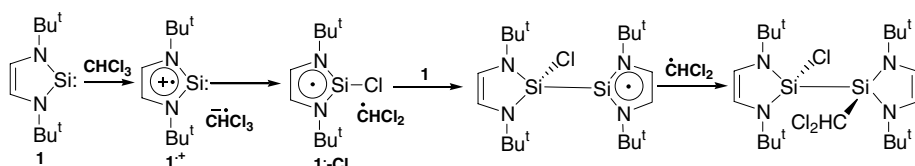Scheme 12.

Scheme 14.

Scheme 15.

observation of rapid disilane formation at room temperature and below. Furthermore, the silylene is assumed to accept electron density from the halogen atom of the organic halide to form **1c**, whereas **1** is known to be a nucleophile. This is exemplified by the fact that a range of metal coordination complexes of **1** have been reported whereas there are no simple donor–acceptor complexes of **1** with bases such as pyridine, NEt₃ or THF (see [48] for reaction of **3** with pyridine).

Matrix isolation studies of the reaction of **1** with CCl₄ revealed formation of the $Cl_3C^\bullet$ radical, indicating that electron transfer may play an important role in these processes [44]. Observation of a small amount ($\approx 1.5\%$) of HCl_2CCCl_2H, arising from $Cl_2CH^\bullet$ radical coupling, in the ^1H and $^{13}C\{^1H\}$ NMR spectra during the thermal reaction of **1** with $CHCl_3$ strongly suggests that these reactions proceed via a radical pathway [45]. One possible radical mechanism is shown in Scheme 17.

Single electron transfer from **1** to the alkyl halide produces the radical cation $\mathbf{1}^{+\bullet}$ which then abstracts Cl^- from the $^-CHCl_3$ species to give the neutral chlorosilyl $\mathbf{1}^\bullet\text{-}Cl$ and $^\bullet CHCl_2$ radicals. There are now two possible reactions which $\mathbf{1}^\bullet\text{-}Cl$ may undergo; either sequential coupling with **1** and $^\bullet CHCl_2$, leading to the disilane, or combination with $^\bullet CHCl_2$ to give the insertion product. The nature of the isolated product appears to depend

Scheme 16.

Scheme 17.

upon the nature of the neutral halocarbon radical in each case. Such a mechanism also explains the reaction of **1** with methyl iodide and iodobenzene, both of which exclusively produce the 1:1 insertion product.

The reactions of **4** with CCl$_4$, CXCl$_3$ (X = Cl or H) yielded products markedly different to those obtained for **1** and **2** [46]. With CXCl$_3$ (X = Cl or H) the dichlorosilane **24** was isolated in high yield, while addition of CH$_3$I exclusively gave the corresponding iodomethylsilane **25**. In contrast, reaction of **4** with CH$_2$Cl$_2$ gave the double insertion product **26** and a small amount of **24**, while reaction with (chloromethyl)cyclopropane produced **24** and the unusual 5-spiro[4.4]nonane derivative **27** (Scheme 18).

As observed in the similar reactions of **1** and **2**, small amounts of the radical coupling products Cl$_3$CCCl$_3$ and HCl$_2$CCCl$_2$H were evident following the reaction of **4** with CCl$_4$ and CHCl$_3$. Their formation, along with that of dichlorosilane **24**, is explained in terms of a radical pathway involving initial complexation of the haloalkane with **4** (this is reasonable since **4** should be a stronger Lewis acid than **1**–**3**). Homolytic scission of the C–Cl bond gives the carbon radical and the chlorinated silyl radical. Chlorine abstraction from the haloalkane by the silyl radical affords dichlorosilane **24**, with recombi-

nation of the carbon radicals giving the observed coupling products.

Production of **26** and **27** is explained by an alternative mechanism involving attack by **4** at a methylene carbon in the initial silylene-alkane complex, with formation of a chlorosilyl anion and a (chloromethyl)silyl cation (for **26**) or a 3-butenylsilyl cation (for **27**). Nucleophilic attack by the chlorosilyl anion affords **26** and **27**, respectively (Scheme 19).

The alkali metal reduction of **4** to produce the anion radical **4**$^{-•}$/M$^+$ has been reported by Kira (M = Na, K, Rb, Cs) [47]. The structure of each **4**$^{-•}$/M$^+$ species was determined by EPR spectroscopy, with **4**$^{-•}$/K$^+$ and **4**$^{-•}$/Rb$^+$ existing as solvent-separated ion pairs but **4**$^{-•}$/Na$^+$ forming a contact ion pair. **4**$^{-•}$/Cs$^+$ rapidly decayed, while **4**$^{-•}$/K$^+$ was found to persist at 213 K but decayed at room temperature ($t_{1/2} \approx 20$ min).
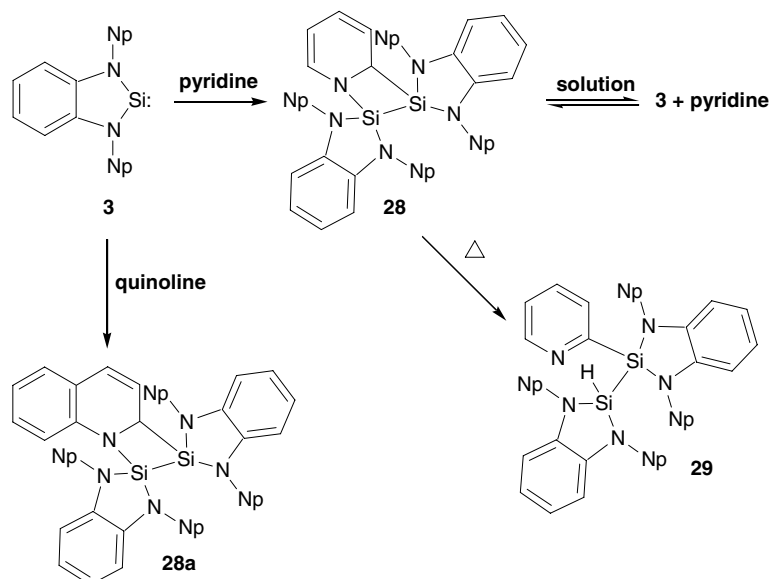
4.2. Reactions with organic compounds

Reaction of **3** with pyridine gave the 1-aza-2,3-disilacyclobutane **28**, which is labile and partially dissociates in solution [48]. The X-ray structure of **28** shows a non-planar C$_5$H$_5$N ring due to the addition of **3** to a pyridine C=N bond. Upon extended heating in benzene,
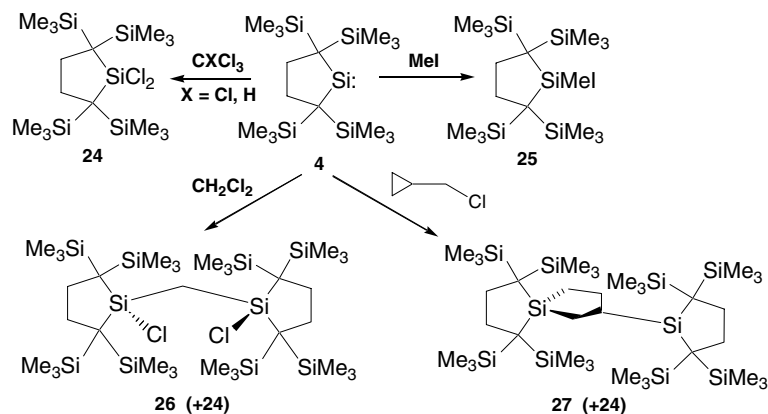
Scheme 18.
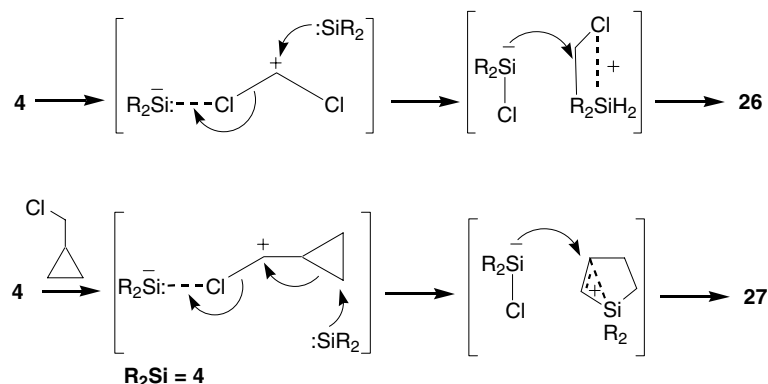
Scheme 19.

Scheme 20.

28 is converted to the thermally stable 2-pyridyldisilane 29 via a 1,3-H migration (Scheme 20). The driving force for this rearrangement (and initial dissociation of 28) is probably the re-aromatization of pyridine. Similar reaction of 3 with quinoline yields the equivalent 1-aza-2,3-disilacyclobutane 28a, which appears to be thermally stable. The overall mechanism for formation of 29 comprises addition of 3 to a C=N bond to give 28, followed by insertion of a further molecule of 3 into 28. 1 and 2 do not react with pyridine.

The [1 + 2] cycloaddition of 3 to the Si=C bond of the transient silene 30, generated in situ from the 1,2-disilacyclobutane 30a in refluxing benzene, afforded the structurally characterized disilirane 31 (Scheme 21) [49]. No reaction was observed at room temperature.

Upon reaction with LiR (R = Me, ^{t}Bu, CH(SiMe$_3$)$_2$, Si(SiMe$_3$)$_3$) 3 inserts into the Li–C or Li–Si bond to give 33–36 [50]. These products likely arise from intramolecular insertion of 3 into the Li–R bond of the intermediate 32 (Scheme 22). Adducts 33–36 are thermally stable and have synthetic potential as silylene transfer reagents, however, a small amount of the disilane [(^{t}Bu)-

Si{(NCH$_2$^{t}Bu)$_2$C$_6$H$_4$-1,2}]$_2$ was observed as a solution decomposition product of 34a.

The insertion of 3 into the N–Li bond of the lithium enamide V (formed by treatment of the bis(silyl)methyl compound IV with AdCN) led to the isolation of the unexpected azatrisilacyclobutane 37. This was assumed to form via LiOMe extrusion from the expected insertion product 37b to give an azadisilacyclopropane 37a, into which a further molecule of 3 inserts to form the observed product (Scheme 23) [51].

The photochemical reactions of 4 with various aromatic compounds have been investigated (Scheme 24) [52]. Irradiation of a combination of 4 and benzene, toluene, m- and p-xylene, or p-disubstituted benzenes at wavelengths >420 nm (n(Si) → 3pπ(Si) λ_{max} = 440 nm for 4), afforded the corresponding silacycloheptatrienes 38a–e, resulting from regioselective insertion of the silylene into the unsubstituted double bond of the aromatic system. No reaction (except the isomerization of 4 to 4a) was observed at elevated temperatures in the dark. Similar reaction of 4 with naphthalene yielded a mixture of the mono- and bis-(silylene) adducts 39 and 40, with the latter being formed by photochemical reaction of 4 with
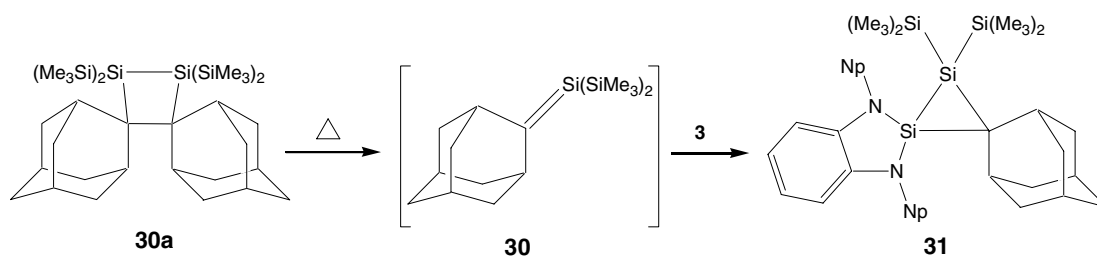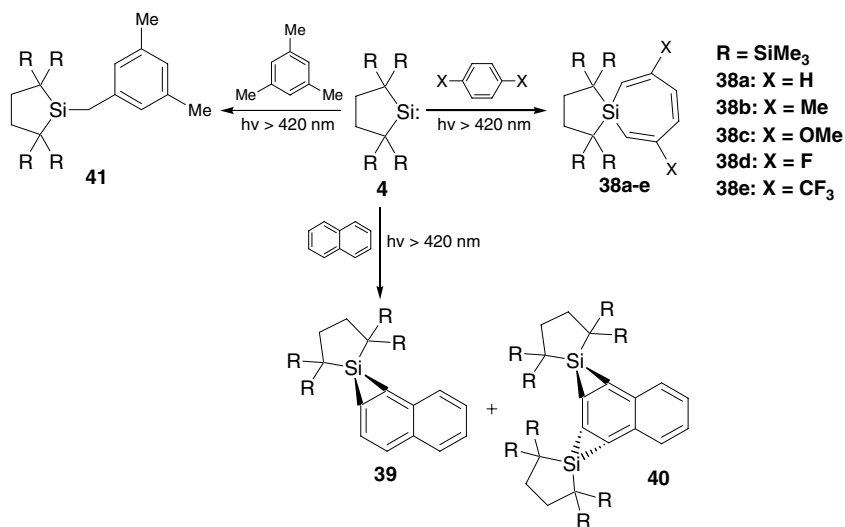

Scheme 21.
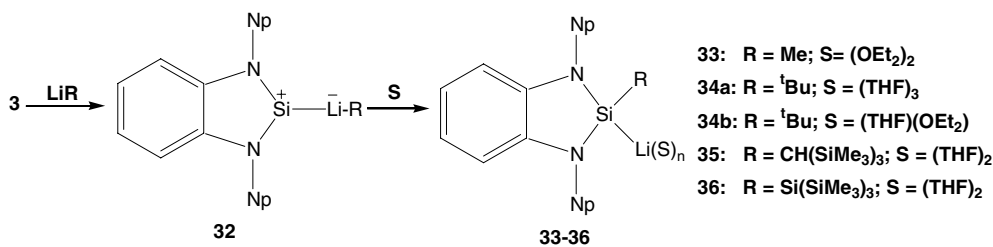
Scheme 22.
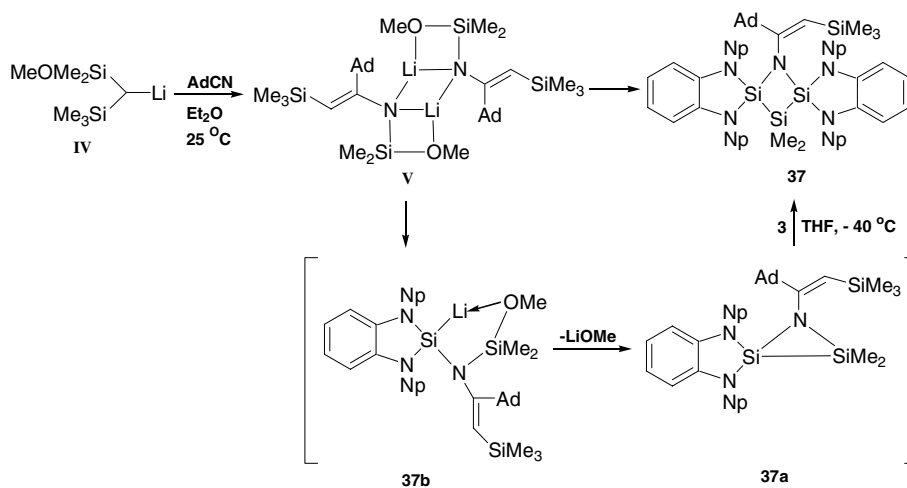
Scheme 23.

Scheme 24.

the thermally unstable **39**. Treatment of **4** with mesitylene under similar conditions gave **41** by insertion of **4** into a C–H bond of a methyl group. All of these reactions were rationalized in terms of a mechanism involving the excited, triplet state of **4** adding to the aromatic system, followed by cyclization and ring-opening to give the observed silacycloheptatriene. Reactions of **4** with bis(trimethyl)acetylene, methanol, ethylene and 2,3-

dimethylbuta-1,3-diene gave the expected addition products [53].

The saturated diaminosilylene **2** is less robust than **1** or **3**, and exists in the solid state as a red, photo- and air-sensitive *Z*-diaminodisilyldisilene, with the colorless silylene present in dilute solution [54]. **2b** is formed by insertion of **2** into the Si–N bond of another molecule of **2**, followed by dimerization, and is the result of a

delicate balance of steric and electronic factors (Scheme 25) [4].

Evidence for the intermediacy of **2a** was obtained by reaction of **2b** with MeOH, which yielded the expected addition product [55]. The direct reaction of the **2b** with 2,4,6-tri-*tert*-butyl-1,3,5-triphosphabenzene (P$_3$C$_3$^{t}Bu$_3$) yielded the crystalline [1 + 4] cycloadduct **42**, thus allowing the first structural authentication of the transient aminosilylsilylene species [56]. Reaction of **3**, **2**, and **1** with P$_3$C$_3$^{t}Bu$_3$ gave similar, structurally characterized [1 + 4] cycloaddition products **43–45**, respectively, with the silylene adding across the P$_3$C$_3$^{t}Bu$_3$ ring. These reactions were shown to be thermally reversible by treatment of **43** with [Mo(CO)$_3$ (norbornadiene)] to afford [Mo(CO)$_3$(η^6-P$_3$C$_3$^{t}Bu$_3$)] and a mixture of *cis-* and *trans-*[Mo(CO)$_4$(**3**)$_2$]. Similar reactions of **44** and **45** were not performed. No reaction was observed between P$_3$C$_3$^{t}Bu$_3$ and the Ge-, Sn- and Pb-analogues of **3**, or the Ge analogue of **1**.

Silylene **3** was recently employed in attempts to prepare a range of 2-phospha-4-silabicyclo[1.1.0]butanes (Scheme 26) [57]. Treatment of **3** with the 1*H*-phosphirenes **46a** and **46b** resulted in the isolation of the first structurally characterized examples of 2,3-dihydro-1,3-phosphasiletes **49a** and **49b**, rather than the target compound. However, DFT calculations and experimental evidence suggest that a 2-phospha-4-silabicyclo[1.1.0]-butane is indeed formed in these reactions, albeit as a transient intermediate (Scheme 26).

Addition of **3** to the C=C bond of **46** leads to the reactive heterobicyclo[1.1.0]butane **47**, which is then at-

tacked by another molecule of **3** at the bridgehead carbon atom. The resultant zwitterion **47a** is stabilized by coordination of **3** to a proximal nitrogen atom, giving thermally stable **48**. Depending upon the nature of the R group attached to the phosphorus atom of **46**, the 2,3-dihydro-1,3-phosphasiletes **49** are formed either directly (**49a**, R = Ph) or by heating a solution of **48** (**49b**, R = Me). Use of the more sterically demanding 1*H*-phosphirene **46c** led to the isolation of the 1,2-dihydro-1,3-phosphasiletes **50a** and **50b** by valance isomerization of the reactive 2-phospha-4-silabicyclo-[1.1.0]butane intermediate.

Reaction of **2** with various azides in hexane gave the spirocyclic silatetraazolines **52**. In addition to the silatetraazoline, the reaction of **2** with *p*-tolyl azide gave a very small amount of the azine-bridged silylene dimer **53** (Scheme 27) [58]. Treatment of **2** with Me$_3$SiN$_3$ gave the azidosilane **54**, as previously observed for the reactions of **1** and **3** with Me$_3$SiN$_3$ in THF [59,60]. Similar reactions of **1** with these azides gave the corresponding silatetrazolines **55** (Fig. 5). It is likely that formation of **52**, **54**, and **55** proceeds via an intermediate iminosilane **51** (shown for **2**) followed by reaction with a further azide molecule to yield the [2 + 3] cycloadducts **52** and **55** or the oxidative product **54**. Electronic effects appear to determine whether the product is a silatetrazoline or an azidosilane, since the latter is obtained from reaction of **1–3** with Me$_3$SiN$_3$ under various reaction conditions.
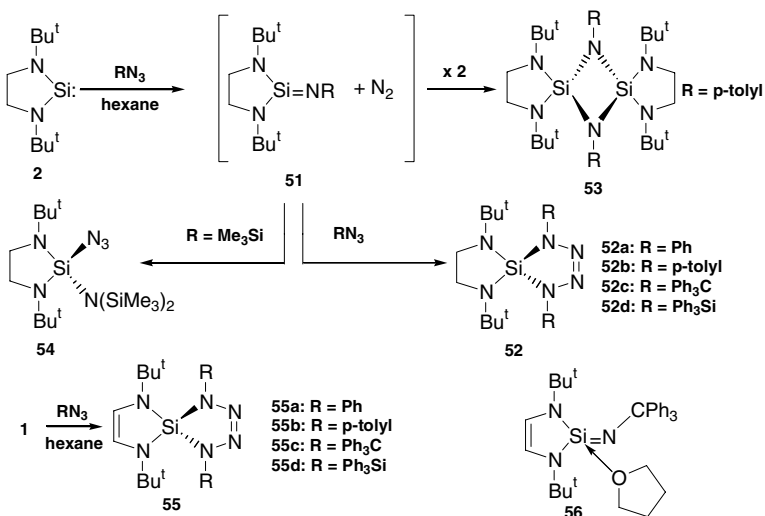
Although the putative base-free iminosilane **51** was not observed directly, the molecular structure of **53** suggests the existence of this species in solution, with the
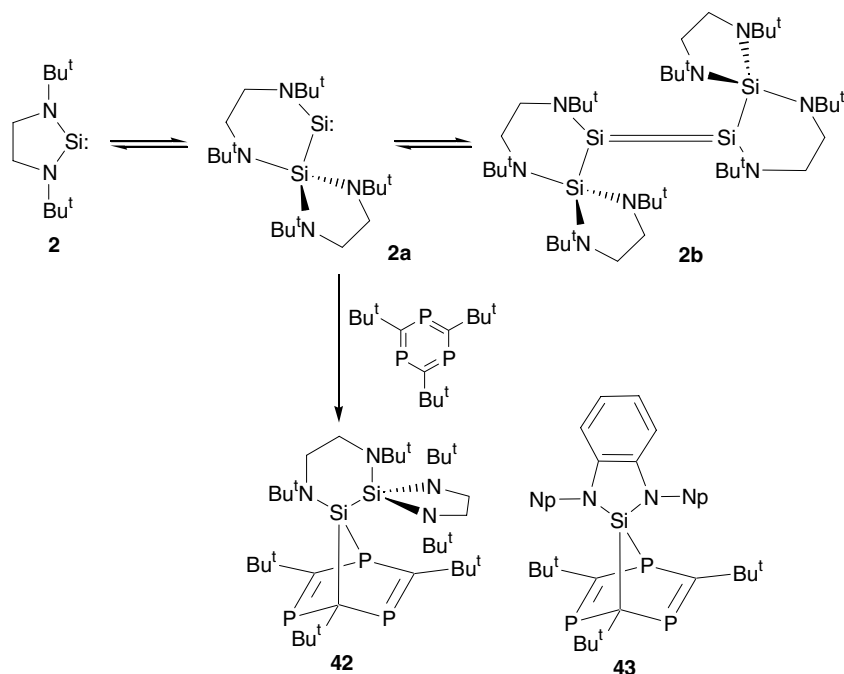
Scheme 25.
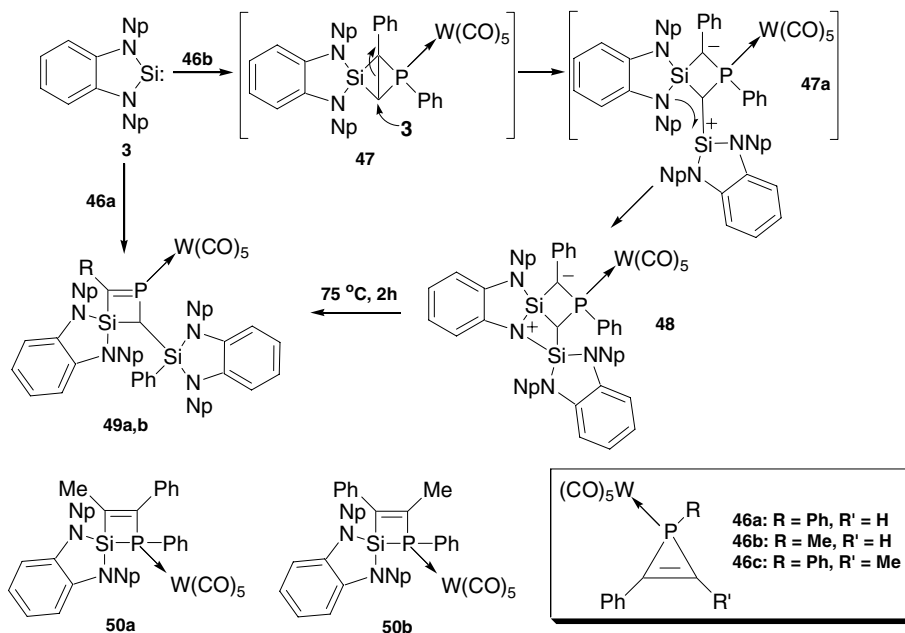
Scheme 26.

Scheme 27.

combination of two such units resulting in the observed product. Addition of a further molecule of RN_3 to **52** is evidently a more facile process, however, since **53** was only isolated as side-product in very low yield. **51** is a plausible intermediate since reaction of **1** with Ph_3CN_3 in THF yielded the base-stabilized iminosilane **56** [60], although repeating the reaction in hexane resulted only in the silatetrazoline **55c** [58]. No similar reactions have been reported for **4**.

1 catalyzes the polymerization of alkenes including ethene, propene, 1-hexene, vinyl chloride, methyl acrylate, styrene, and terminal alkynes [61]. The polymers produced are highly cross-linked, although the mechanism of this reaction is currently unclear.

4.3. Reactions with inorganic and organometallic compounds

4.3.1. Main group compounds

Reaction of **2** with one equivalent of potassium gives the disilanyl dianion 57^{2-} which was trapped with alcohol or water to give the corresponding 1,2-dihydride [62]. Similar reaction of **2** with two equivalents of potassium yields the silyl dianion 58^{2-}, which is stable in THF solution at -20 °C but slowly deprotonates THF at 25 °C ($t_{1/2} \approx 3$ h) to form the hydrosilyl monoanion 58^- which can be trapped by electrophiles (Scheme 28).

Reduction of **1** does not produce anionic products, although theoretical calculations suggest that the
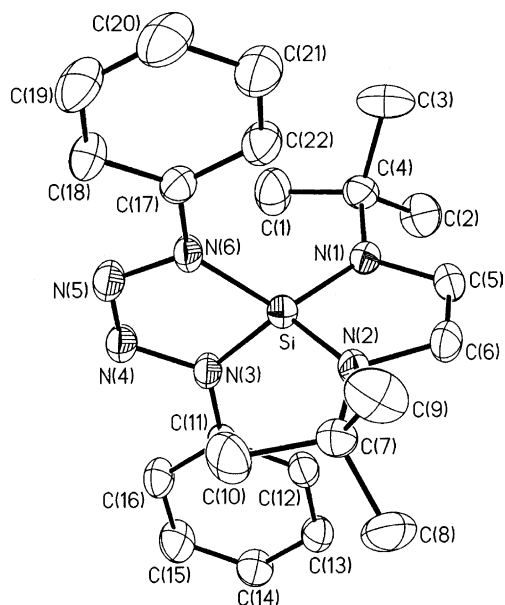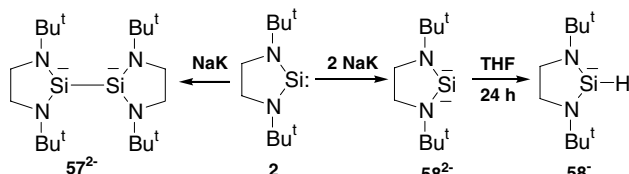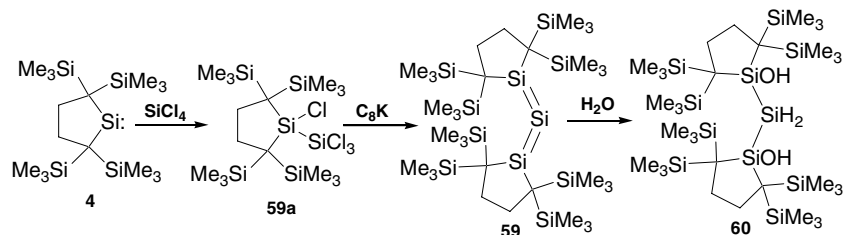
Fig. 5. Crystal structure of **55a** [58].

enthalpy of electron attachment to **1** is slightly more favorable than that for **2** (-12.1 kJ mol^{-1} vs. -11.3 kJ mol^{-1}, respectively) [62]. A possible explanation for this is that alkali metal reduction of **1** breaks Si–N bonds to eventually liberate the diimine ^{t}BuN=CH–CH=N^{t}Bu, which reacts further with **1** to form a spirocyclic compound. A similar reaction does not readily occur with **2**, possibly because Si–N bond cleavage does not produce a neutral product.

The Kira group recently described **59**, the first example of a thermally stable, crystalline, silicon-based allene analogue [63]. This notable species was prepared in two steps starting with oxidative insertion of **4** into SiCl$_4$ to

produce a tetrachlorodisilane derivative **59a**, followed by low temperature KC$_8$ reduction (Scheme 29).

The X-ray crystal structure of **59** reveals that the trisilaallene Si=Si=Si skeleton is significantly bent, in contrast to linear carbon allenes. Of further note is the fact that the central silicon atom readily rotates around the molecular axis leading to temperature-dependant dynamic disorder over four positions in the crystal structure (Fig. 6).

Ab inito molecular orbital calculations suggest that this bent arrangement is brought about by a combination of the steric demand and the electronic properties of the dialkyl silylene moieties. ^{1}H, ^{13}C and ^{29}Si NMR data indicate that the solid-state structure is retained in solution. Treatment of the silaallene with water gave the expected 1,3-dihydroxytrisilane **60** [63]. The germanium analogue of **59** has been reported recently [64]. There are as yet no reports of metal coordination complexes of **4**.

The reaction of **1** with the highly electrophilic diamino phosphenium species [P(NCy$_2$)$_2$]$^+$[AlCl$_4$]$^-$ (Cy = cyclohexyl) at -80 °C was recently reported [65]. The target species, the silylene phosphonium ion **61**, was not directly observed but instead postulated as an intermediate to which a chloride ion is transferred (from the [AlCl$_4$]$^-$ anion), with formation of the observed phosphino(chloro)silane **62** (Scheme 30). Attempts to isolate **62** resulted in hydrolytic scission of the Si–P bond with formation of hydridochlorosilane **63** and bis(dicyclohexylamino)phosphine oxide. These products would not be expected on consideration of the relative electronegativity of the Si and P atoms (1.7 and 2.1, respectively, on the Allred–Rochow scale) hence interaction with the phosphenium cation must alter the nature of the silicon atom in the intermediate **61** from nucleophilic to primarily electrophilic. DFT calculations upon the model compound indicate that the lone pair of the silylene is donated into the vacant, phosphorus-based orbital of the phosphenium ion, suggesting that it is more appropriate to describe **61** as a phosphanylsilyl cation [65].

4.3.2. Transition metal compounds

Whereas the use of transition metal complexes featuring N-heterocyclic carbene ligands in organic synthesis and catalysis is currently an area of heavy research activ-
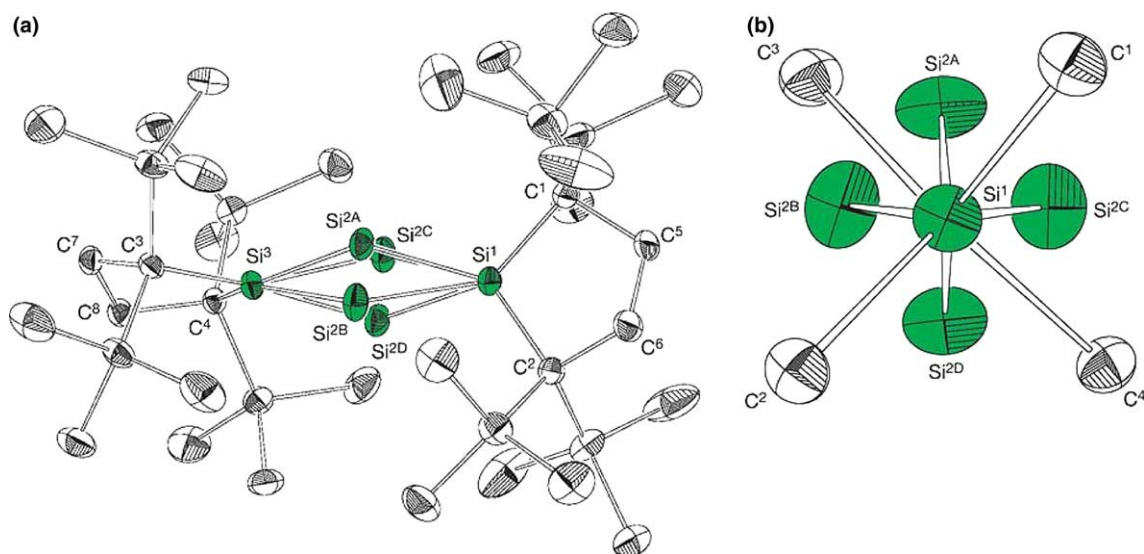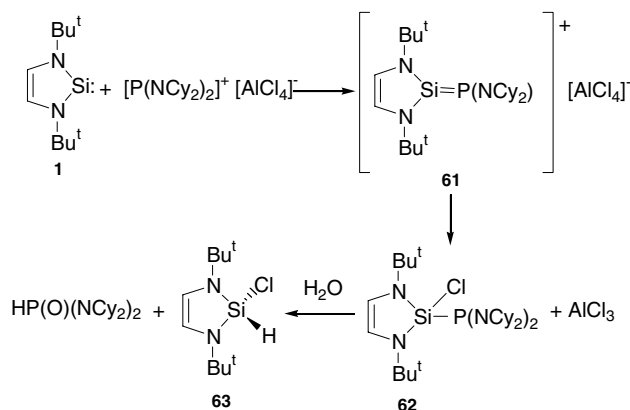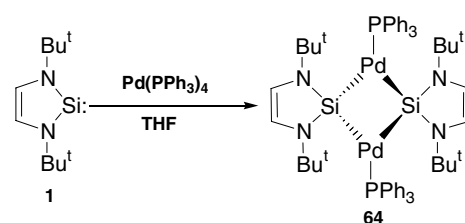

Scheme 28.

Scheme 29.

Fig. 6. (a) Crystal structure of **59**. (b)View along the Si(1)–Si(3) axis. Reprinted from [63]. Copyright Nature Publishing Group.
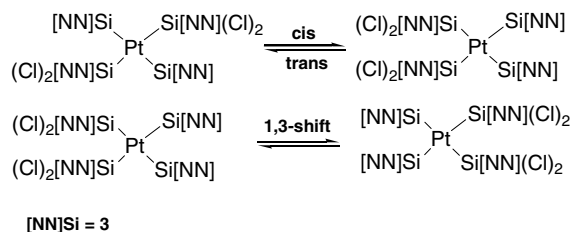

Scheme 30.

Scheme 31.

ity [66], very little work has been done concerning the application of analogous silylene complexes to these areas. To date only two such examples have been reported, both concerning the structurally characterized dinuclear Pd(0) complex **64**, in which **1** bridges two 14-electron Pd(0) atoms (Scheme 31) [67]. This complex, like the homoleptic, mononuclear bis(carbene) analogue [68], was found to be catalytically active in the Suzuki [67] and Stille [69] cross-coupling reactions. In some cases, **64** gives higher yields of the desired coupled product with less homo-coupled side products.

Herrmann et al. [70] described a study of Pd(P^{t}Bu$_3$)$_2$, Pd(COD)$_2$ and Pd(COD)(CH$_3$)$_2$ complexes of **1** and **2**, where both labile homoleptic and bridged Pd(0) species were observed (COD=1,8-cyclooctadiene). Reaction of Pd(P^{t}Bu$_3$)$_2$ with an excess of **1** or **2** gave the homoleptic complexes [Pd(**1**)$_3$] (**65**), [Pd(**1**)$_2$]$_2$ (**66**), and [Pd(**2**)$_4$] (**67**) in solution (as judged by ^{1}H, ^{31}P and ^{29}Si NMR spectroscopy), although these compounds were unstable in the

presence of free phosphane thus only the corresponding dinuclear, μ-silylene complexes [Pd(P^{t}Bu$_3$)(**1**)]$_2$ (**68**) and [Pd(P^{t}Bu$_3$)(**2**)]$_2$ (**69**) were isolated and structurally characterized. The Pd–Si bond distances and angles in **68** and **69** are very similar to those reported for **64** [67]. Treatment of excess **1** and **2** with Pd(COD)$_2$ produced complicated mixtures, while similar reaction with Pd(COD)Me$_2$ produced **65** and **67** along with (Me)$_2$Si(^{t}BuNCHCHCHN^{t}Bu) and the disilane [MeSi (^{t}BuNCHCHCHN^{t}Bu)]$_2$, respectively.

The d^{10} metal complexes [Ni(**3**)$_4$], [Pt(PPh$_3$)(**3**)$_3$], and [CuI(PPh$_3$)$_2$(**3**)] (**70**) were obtained from the substitution reactions of **3** with [Ni(COD)$_2$], [Pt(PPh$_3$)$_4$], and [Cu(I)(PPh$_3$)$_3$], respectively [71]. **70** is the first reported example of a copper complex of **1**–**4**, and contains the Cu(II) atom in a distorted tetrahedral environment with a Cu–Si bond distance of 2.289(4) Å. The complex decomposed in CDCl$_3$, and fast dissociative exchange in C$_6$D$_6$ precluded the collection of ^{29}Si{^{1}H} NMR data.

Similar reaction of **3** with [MCl$_2$(PPh$_3$)$_2$] (M=Pt, Pd, Ni) gave either the square planar d^8 complexes trans-[Pt(**3**)$_2$(**3**-Cl$_2$)$_2$] (**71**) and trans-[Pd(**3**)$_2$(**3**-Cl$_2$)$_2$], or the d^{10} species [Ni(**3**)$_n$(PPh$_3$)$_{4-n}$] (**72**) and **3**-Cl$_2$ [71]. The composition of **72** was dependant upon reaction stoichiometry. Variable temperature NMR measurements

Scheme 32.

Scheme 33.

show that **71** undergoes fluxional processes in solution, including solvent dependant *cis–trans* isomerism (two rotamers of the *trans* isomer were detected by ^{29}Si NMR spectroscopy) and Si → Si 1,3-shift of Cl$^-$ (Scheme 32).

The synthesis of the *cis*- and *trans*-[Mo(CO)$_4$(**3**)$_2$] complexes was outlined in section 4.2 ([56]). The *cis*-isomer is the first example of an octahedral bis[bis(amino)silylene] metal carbonyl complex with the ligands in such an arrangement. The *trans*-isomer was crystallographically characterized.

The reaction of **1** with [Cp*Ru(μ$_3$-Cl)]$_4$(Cp* = C$_5$Me$_5$) gave the dark blue 16-electron complex [Cp*Ru(**1**)Cl] **73** in (Scheme 33) [72].

This compound further reacted with primary silanes to give the adducts [(Cp*Ru)$_2$(H)(μ-H)(μ,η^2-HSiRCl)(μ,η^2-Cl(**1**))] (**74**) (R = Ph or *n*-C$_6$H$_{13}$), where the Si(II) is oxidized to Si(IV). Treatment of [Cp*Ru(CH$_3$CN)$_3$][OTf] with **1** gave [Cp*Ru(**1**)(CH$_3$CN)$_2$][OTf] (**75**), which was converted to the remarkable η^5-silylene complex [Cp*Ruη^5:η^1-(**1**)Cp*Ru(CH$_3$CN)$_2$][OTf]$_2$ (**76**) by heating a THF solution to 80 °C (Scheme 34).

This species provides the first evidence that, under appropriate conditions, **1** may function as a η^5-ligand (although no structural data were reported, the overall connectivity of **76** was confirmed by X-ray crystallography). Similar reaction of **1** with [Cp*Ru(μ-OMe)]$_2$ gave complicated mixtures according to NMR spectroscopy [72].

The samarocene complex [Cp$_2^*$Sm(**1**)] (**77**) has recently been isolated from the reaction of Cp$_2^*$Sm with **1** in PhMe (Scheme 35) [73]. In contrast, no reaction was observed between **1** and Cp$_2^*$Sm(THF)$_2$, and addition of THF to a C$_6$D$_6$ solution of **77** gave only
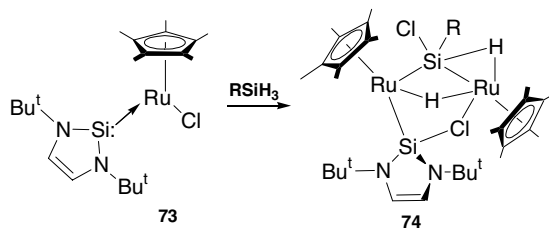
Cp$_2^*$Sm(THF)$_2$. The X-ray crystal structure of **77** shows **1** to be asymmetrically bound, with one of the *tert*-butyl groups of **1** located much closer to the central Sm(II) atom than the other. **77** represents only the third example of a lanthanide metal complex featuring an *N*-heterocyclic silylene ligand, the others being [Ln(η^5-Cp)$_3$(**3**)] (Ln = Y, Yb; Cp = C$_5$H$_5$) [74].

Reaction of **1** with 0.25 equivalents of the coordinatively unsaturated Ru complex **78** gave **79**, a rare example of a *trans*-diphosphane complex (Scheme 36) [75].

Two related mechanistic routes to **79** were proposed (Scheme 37). Path A involves initial coordination of **1** to give **VI**, which may trigger oxidative addition of a C–H bond of the diphosphane backbone to the metal, accompanied by silylene insertion into the Ru–Cl bond (**VII**). **79** is then formed by reductive elimination of **63** and coordination of a second molecule of **1**. An alternative route (Path B) involves the direct insertion of **1** into the Ru–Cl to give a four-coordinate Ru atom (**VIII**), followed by elimination and coordination steps similar to Path A.

Treatment of **79** with CO displaces **1** with formation of three isomeric ruthenium-bis(carbonyl) adducts, while reaction of **79** with H$_2$ containing adventitious
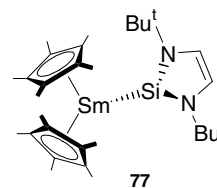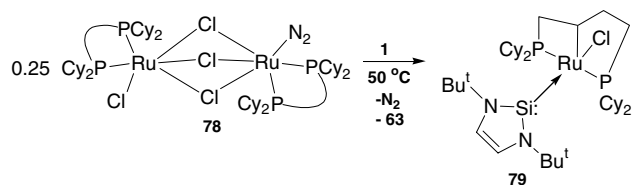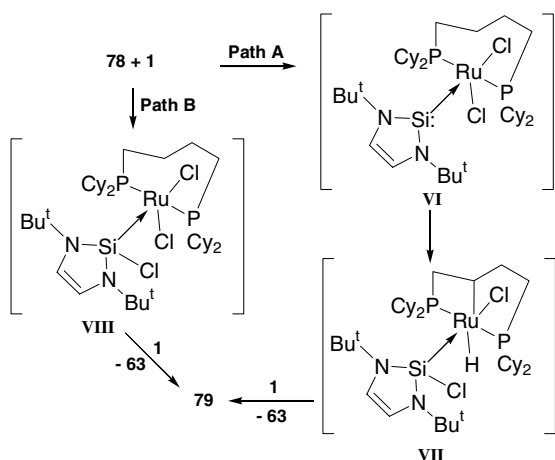

Scheme 35.
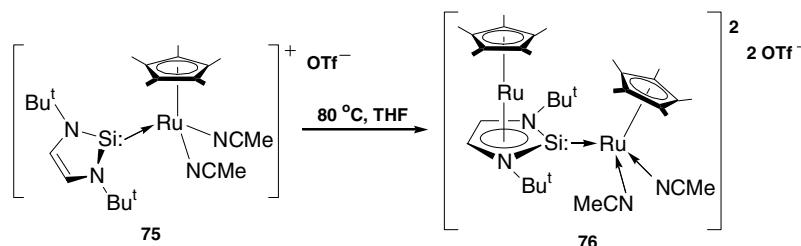
Scheme 34.

Scheme 36.

moisture leads to the isolation of the ruthenium-hydride-H$_2$ and the dimeric siloxane **81** (Scheme 38).

A DFT study upon model Me–Pd(II) complexes of N-heterocyclic silylenes and germylenes **IX** has implications for the use of **1** and related germanium species in certain catalytic processes (Scheme 39) [76]. These calculations reveal a much lower activation barrier for methyl migration from Pd to the coordinated silylene or germylene than in the corresponding carbene complex, with

elimination of the silecenium cation **X** occurring in some cases.

The authors suggest that, where metal-hydrocarbyl species are involved in a catalytic cycle, such facile migrations might lead to reduction of the metal and decomposition of the catalytic complex, thus limiting the use of **1** as an ancillary ligand [76].

Okazaki et al. [77] recently reviewed the chemistry of transition metal complexes featuring acyclic, base-stabilized silylenes.

5. Conclusions and prospects

The chemistry of stable silylenes has seen major developments during the past five years. Many new reactions of nitrogen-stabilized silylenes have been described, leading to a variety of hitherto-unknown structures. The first silylene (**4**) stabilized only by steric effects has been reported [7]. Studies of the stable silylenes as electron donors to transition metals and lanthanides show that the silylenes are unique ligands, producing in many cases previously unknown types of ligand–metal complexes.

Much in this field, however, remains unknown. The number of stable silylenes is still very small. Among the hundreds of stable silylenes which now seem possible, only about seven are yet known, and only **1**–**4** have been studied in any depth. The radical chemistry of stable silylenes is just beginning to be investigated, and almost nothing is known of their excited-state chemistry. The use of silylene–metal complexes (and of stable silylenes themselves) as catalysts is promising and clearly deserving of further study. Finally, very little has yet been done to elucidate mechanisms of the many new reactions of these molecules. Thus a great deal remains for chemists to do in this area in the future.
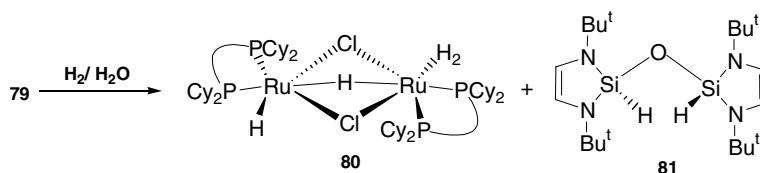
Scheme 37.
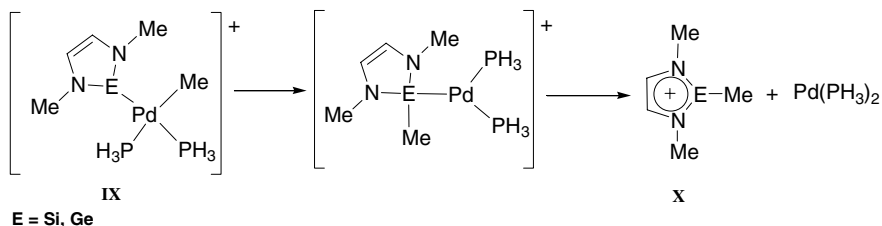
Scheme 38.

Scheme 39.

References

[1] P.P. Gaspar, R. West, in: Z. Rappoport, Y. Apeloig (Eds.), The Chemistry of Organic Silicon Compounds, vol. 2, Wiley, Chichester, 1998, p. 2463 (Chapter 43).

[2] A.J. Arduengo III, R.L. Harlow, M. Kline, J. Am. Chem. Soc. 113 (1991) 361.

[3] (a) M. Denk, R. Lennon, R. Hayashi, R. West, A.V. Belyakov, H.P. Verne, A. Haaland, M. Wagner, N. Metzler, J. Am. Chem. Soc. 116 (1994) 2691;
(b) R. West, M. Denk, Pure Appl. Chem. 68 (1996) 785;
(c) B. Gehrhus, M.F. Lappert, J. Heinicke, R. Boese, D. Bläser, J. Chem. Soc., Chem. Commun. 1931 (1995).

[4] T.A. Schmedake, M.P. Haaf, Y. Apeloig, T. Müller, S. Bukalov, R. West, J. Am. Chem. Soc. 121 (1999) 9479.

[5] (a) B. Gehrhus, M.F. Lappert, J. Organomet. Chem. 617 (2001) 209;
(b) T.A. Schmedake, M. Haaf, R. West, Acc. Chem. Res. 33 (2000) 704.

[6] The chemistry of N-heterocyclic germylenes and related compounds has recently been reviewed: O. Kühl, Coord. Chem. Rev. 248 (2004) 411.

[7] M. Kira, S. Ishida, T. Iwamoto, C. Kabuto, J. Am. Chem. Soc. 121 (1999) 9722.

[8] M. Kira, S. Ishida, T. Iwamoto, M. Ichinohe, C. Kabuto, L. Ignatovich, H. Sakurai, Chem. Lett. (1999) 263.

[9] D.H. Harris, M.F. Lappert, J. Chem. Soc., Chem. Commun. (1974) 895;
M.S.J. Gynane, D.H. Harris, M.F. Lappert, P.P. Power, P. Riviere, M. Riviere-Baudet, J. Chem. Soc., Dalton Trans. (1977) 2004.

[10] G.-H. Lee, T. Müller, R. West, J. Am. Chem. Soc. 125 (2003) 8114.

[11] B. Gehrhus, P. Hitchcock, L. Zhang, Angew. Chem., Int. Ed. Engl. 43 (2004) 1124.

[12] N.J. Hill, R. West, unpublished results.

[13] J. Heinicke, A. Oprea, M.K. Kinermann, T. Kárpáti, L. Nyulászi, T. Veszprémi, Chem. Eur. J. 4 (1998) 541.

[14] H.H. Karsch, P.A. Schlueter, F. Bienlein, M. Herker, E. Witt, A. Sladek, M. Heckel, Z. Anorg. Allg. Chem. 624 (1998) 295.

[15] M.E. Lee, H.M. Cho, C.H. Kim, W. Ando, Organometallics 20 (2001) 1472.

[16] D.F. Moser, I.A. Guzei, R. West, Main Group Met. Chem. 24 (2001) 811.

[17] J.S. Becker, R.J. Staples, R.G. Gordon, Cryst. Res. Technol. 39 (2004) 85.

[18] W.A. Herrmann, M. Denk, J. Behm, W. Scherer, F.-R. Klingan, H. Bock, B. Solouki, M. Wagner, Angew. Chem., Int. Ed. Engl. 31 (1992) 1485.

[19] A.J. Arduengo III, H. Bock, H. Chen, M. Denk, D. Dixon, J. Green, W.A. Herrmann, N. Jones, M. Wagner, R. West, J. Am. Chem. Soc. 116 (1994) 6641.

[20] C. Heinemann, T. Müller, Y. Apeloig, H. Schwarz, J. Am. Chem. Soc. 118 (1996) 2023.

[21] R. West, J.J. Buffy, M. Haaf, T. Müller, B. Gehrhus, M.F. Lappert, Y. Apeloig, J. Am. Chem. Soc. 120 (1998) 1639.

[22] L.A. Leites, S.S. Buklalov, M. Denk, R. West, M. Haaf, J. Mol. Struct. 550 (2000) 329.

[23] P.P. Shorygin, Pure Appl. Chem. 4 (1962) 87.

[24] L.A. Leites, S.S. Bukalov, A.V. Zabula, I.A. Garbuzova, D.F. Moser, R. West, J. Am. Chem. Soc. 126 (2004) 4114.

[25] J. Oláh, T. Veszprémi, J. Organomet. Chem. 686 (2003) 112.

[26] M.-D. Su, S.-Y. Chu, Inorg. Chem. 38 (1999) 4819.

[27] J. Oláh, F. De Profit, T. Veszprémi, P. Geerlings, J. Phys. Chem. A 108 (2004) 490.

[28] T. Veszprémi, L. Nyulászi, B. Hajgato, J. Heinicke, THEOCHEM 431 (1998) 1.

[29] T. Müller, J. Organomet. Chem. 686 (2003) 251.

[30] L. Pause, M. Robert, J. Heinicke, O. Kühl, J. Chem. Soc., Perkin Trans. 2 (2001) 1383.

[31] A. Dhiman, J.Y. Becker, T. Müller, R. West, Organometallics, in press.

[32] M. Denk, J.C. Green, N. Metzler, M. Wagner, J. Chem. Soc., Dalton Trans. (1994) 1475.

[33] T. Veszprémi, L. Nyulászi, T. Kárpáti, J. Phys. Chem. A 100 (1996) 6262.

[34] T. Veszprémi, Adv. Mol. Struct. Res. 6 (2000) 267.

[35] W.W. Schoeller, D. Eisner, Inorg. Chem. 43 (2004) 2585.

[36] I.S. Orlov, M.P. Egorov, O.M. Nefedov, D.F. Moser, R. West, unpublished results.

[37] B. Tumanskii, P. Pine, Y. Apeloig, N.J. Hill, R. West, J. Am. Chem. Soc. 126 (2004) 7786.

[38] A. Naka, N.J. Hill, R. West, Organometallics (2004), submitted.

[39] T. Iwamoto, H. Masuda, S. Ishida, C. Kabuto, M. Kira, J. Am. Chem. Soc. 125 (2003) 9300.

[40] T. Iwamoto, H. Masuda, S. Ishida, C. Kabuto, M. Kira, J. Organomet. Chem. 689 (2004) 1337.

[41] D.F. Moser, T. Bosse, J. Olson, J.L. Moser, I.A. Guzei, R. West, J. Am. Chem. Soc. 124 (2002) 4186.

[42] M.-D. Su, J. Am. Chem. Soc. 125 (2003) 1714.

[43] M.-D. Su, Chem. Phys. Lett. 374 (2003) 385.

[44] J. Glathaar, G. Meier, R. West, unpublished work.

[45] A. Naka, R. West, unpublished work.

[46] S. Ishida, T. Iwamoto, C. Kabuto, M. Kira, Chem. Lett. (2001) 1102.

[47] S. Ishida, T. Iwamoto, M. Kira, J. Am. Chem. Soc. 125 (2003) 3212.

[48] B. Gehrhus, P. Hitchcock, J. Organomet. Chem. 689 (2004) 1350.

[49] B. Gehrhus, P.B. Hitchcock, Organometallics 23 (2004) 2848.

[50] X. Cai, B. Gehrhus, P.B. Hitchcock, M.F. Lappert, J.C. Slootweg, J. Organomet. Chem. 643–644 (2002) 272.

[51] F. Antolini, B. Gehrhus, P.B. Hitchcock, M.F. Lappert, Angew. Chem., Int. Ed. 41 (2002) 2568.

[52] M. Kira, S. Ishida, T. Iwamoto, C. Kabuto, J. Am. Chem. Soc. 124 (2002) 3830.

[53] M. Kira, Pure Appl. Chem. 72 (2000) 2333.

[54] M. Haaf, T.A. Schmedake, B.J. Paradise, R. West, Can. J. Chem. 78 (2000) 1526.

[55] T.A. Schmedake, Ph.D. Thesis, University of Wisconsin–Madison, USA, 2000.

[56] S.B. Clendenning, B. Gehrhus, P. Hitchcock, D.F. Moser, J. Nixon, R. West, J. Chem. Soc., Dalton Trans. (2002) 484.

[57] J.C. Slootweg, F.J.J. de Kanter, M. Schakel, A.W. Ehlers, B. Gehrhus, M. Lutz, A.M. Mills, A.L. Speck, K. Lammertsma, Angew. Chem., Int. Ed. 43 (2004) 3474.

[58] N.J. Hill, D.F. Moser, R. West, unpublished work.

[59] B. Gehrhus, P.B. Hitchcock, M.F. Lappert, Z. Anorg. Allg. Chem. 627 (2001) 1048.

[60] M. Denk, R.K. Hayashi, R. West, J. Am. Chem. Soc. 116 (1994) 10813.

[61] R. West, D.F. Moser, M.P. Haaf, PCT Int. Appl. (2002).

[62] R. West, T.A. Schmedake, M. Haaf, J. Becker, T. Müller, Chem. Lett. 30 (2001) 68.

[63] S. Ishida, T. Iwamoto, C. Kabuto, M. Kira, Nature (London) 421 (2003) 725.

[64] M. Kira, S. Ishida, T. Iwamoto, Chem. Record 4 (2004) 243.

[65] R. Pietschnig, Chem. Commun. (2004) 546.

[66] W.A. Herrmann, Angew. Chem., Int. Ed. 41 (2002) 1290;
T.M. Trnka, R.H. Grubbs, Acc. Chem. Res. 34 (2001) 18.

[67] A. Fürstner, H. Krause, C.W. Lehmann, Chem. Commun. (2001) 2372.

[68] L.R. Titcomb, S. Caddick, F.G.N. Cloke, D.J. Wilson, D. McKerrer, Chem. Commun. (2001) 1388.

[69] K. Lassen, M. Sangi, M.P. Haaf, unpublished work.

[70] W.A. Herrmann, P. Härter, C.W.K. Gstöttmayr, F. Bielert, N. Seeboth, P. Sirsch, J. Organomet. Chem. 649 (2002) 141.

[71] A.G. Avent, B. Gehrhus, P.B. Hitchcock, M.F. Lappert, H. Maciejewski, J. Organomet. Chem. 686 (2003) 321.

[72] J.M. Dysard, T.D. Tilley, Organometallics 19 (2000) 4726.

[73] W.J. Evans, J.M. Perotti, J.W. Ziller, D.F. Moser, R. West, Organometallics 22 (2003) 1160.

[74] X. Cai, B. Gehrhus, P.B. Hitchcock, M.F. Lappert, Can. J. Chem. 78 (2000) 1484.

[75] D. Amoroso, M. Haaf, G.P.A. Yap, R. West, D.E. Fogg, Organometallics 21 (2002) 534.

[76] D.S. McGuinness, B.F. Yates, K.J. Cavell, Organometallics 21 (2002) 5408.

[77] M. Okazaki, H. Tobita, H. Ogino, J. Chem. Soc., Dalton Trans. (2003) 493.